Flexible Optical Waveguides for Uniform Periscleral Cross-Linking

Flexible Optical Waveguides for Uniform Periscleral Cross-Linking

Sheldon J. J. Kwok,[1,2] Moonseok Kim,[1] Harvey H. Lin,[1] Theo G. Seiler,[1,3] Eric Beck,[1] Peng Shao,[1] Irene E. Kochevar,[1] Theo Seiler,[3] and Seok-Hyun Yun[1,2]

[1]Harvard Medical School and Wellman Center for Photomedicine, Massachusetts General Hospital, Boston, Massachusetts, United States
[2]Harvard-MIT Health Sciences and Technology, Massachusetts Institute of Technology, Cambridge, Massachusetts, United States
[3]Institute for Refractive and Ophthalmic Surgery (IROC), Zurich, Switzerland

Correspondence: Seok-Hyun Yun, Harvard University, 65 Landsdowne Street UP-525, Cambridge, MA 02139, USA; syun@hms.harvard.edu.

SJJK and MK contributed equally to the work presented here and should therefore be regarded as equivalent authors.

Submitted: January 25, 2017
Accepted: April 11, 2017

Citation: Kwok SJJ, Kim M, Lin HH, et al. Flexible optical waveguides for uniform periscleral cross-linking. *Invest Ophthalmol Vis Sci*. 2017;58:2596–2602. DOI:10.1167/iovs.17-21559

Purpose. Scleral cross-linking (SXL) with a photosensitizer and light is a potential strategy to mechanically reinforce the sclera and prevent progressive axial elongation responsible for severe myopia. Current approaches for light delivery to the sclera are cumbersome, do not provide uniform illumination, and only treat a limited area of sclera. To overcome these challenges, we developed flexible optical waveguides optimized for efficient, homogeneous light delivery.

Methods. Waveguides were fabricated from polydimethylsiloxane elastomer. Blue light (445 nm) is coupled into the waveguide with an input fiber. Light delivery efficiency from the waveguide to scleral tissue was measured and fit to a theoretical model. SXL was performed on fresh porcine eyes stained with 0.5% riboflavin, using irradiances of 0, 25, and 50 mW/cm^2 around the entire equator of the eye. Stiffness of scleral strips was characterized with tensiometry.

Results. Light delivery with a waveguide of tapered thickness (1.4–0.5 mm) enhanced the uniformity of light delivery, compared to a flat waveguide, achieving a coefficient of variation of less than 10%. At 8% strain, sclera cross-linked with the waveguides at 50 mW/cm^2 for 30 minutes had a Young's modulus of 10.7 ± 1.0 MPa, compared to 5.9 ± 0.5 MPa for no irradiation, with no difference in stiffness between proximally and distally treated halves. The stiffness of waveguide-irradiated samples did not differ from direct irradiation at the same irradiance.

Conclusions. We developed flexible waveguides for periscleral cross-linking. We demonstrated efficient and uniform stiffening of a 5-mm-wide equatorial band of scleral tissue.

Keywords: photo–cross-linking, optical waveguide, sclera reinforcement, myopia control

Myopia is a rapidly growing visual disorder, which could affect 2.5 billion people—one-third of the world's population—by 2020.[1] Patients with severe myopia are highly susceptible to other serious problems such as retinal detachment, glaucoma, and cataract.[2] Since the severity of myopia increases with earlier onset, strategies to control myopia progression in at-risk children and young patients with high myopia are of great interest. Although scleral deformities are thought to be in response to aberrant retinal signaling, pathologic changes in the sclera have been identified as an important feature in the early development of myopia and considered possible targets for preventive therapy. In particular, studies[3–5] have suggested that matrix remodeling of the sclera plays an active role leading to thinning and biomechanical weakening of scleral tissue, and subsequent axial lengthening of the vitreous chamber. A promising strategy to stabilize the axial length and thereby frustrate myopia development is to mechanically reinforce the sclera. Surgical reinforcement of the posterior sclera with mechanically stiffer donor grafts or artificial biological materials has been performed on patients with severe myopia with mixed success.[6–8] The efficacy of scleral reinforcement surgeries is controversial, and its use remains limited outside Russia and China, owing to low efficacy, high invasiveness, serious complications, and need for healthy scleral donor tissue.[9,10]

Corneal collagen cross-linking is a minimally invasive, successful treatment already adopted in the clinic to arrest the progression of keratoconus primarily by improving the mechanical stability of corneal tissues.[11] Collagen cross-linking is an attractive technique for strengthening the sclera to prevent the progression of pathologic myopia. Light-activated photosensitizers induce intermolecular cross-links between neighboring collagen molecules, strengthening the collagen network and enhancing tissue rigidity. Scleral cross-linking (SXL) has been demonstrated in several animal models,[12–17] as well as ex vivo human sclera,[18] most commonly by using riboflavin in conjunction with UV-A (360–370 nm) or blue light. Target regions for SXL treatment include the equatorial sclera, which is weakened in the early stages of myopia, and the posterior pole, which is affected later and more dramatically.[19]

Unlike the cornea, the anatomic shape of the sclera poses significant technical challenges for photo-mediated cross-linking. The equatorial sclera spans a long length (6–8 cm) and is not readily accessible by external laser illumination. A

light-delivery apparatus must be safely introduced and operated deep in the eye socket to deliver light to the relatively large target region with sufficient irradiance. Homogeneous light distribution around the eye globe is another critical requirement for uniform stiffening to prevent asymmetric changes to eye shape. Previously described approaches for light delivery typically involve invasive and time-consuming dissection of surrounding soft tissues, such as attached extraocular muscles, to expose scleral tissue.[20] For example, recent approaches involve rotating the eye to expose target regions along the equator,[12,13,21] or at the posterior pole,[14] to an external light source or fiber-optic probe. The area of each of these irradiation zones ranges from 10 to 100 mm^2 and is limited by the size of the probe that can be safely inserted. To irradiate a larger area, one alternative approach uses miniature light-emitting diodes (LEDs) wrapped around the eyeball,[22] but inhomogeneous light distribution, poor mechanical flexibility, and risk of thermal damage to tissues caused by LED heat generation limits their applicability.

Biomaterial waveguides with attractive properties such as flexibility, biocompatibility, and efficient light delivery are increasingly used to deliver light into tissues for biomedical applications.[23] In this study, we describe the development of fiber-coupled, polymer waveguides for homogeneous periscleral cross-linking. Our waveguides are well suited for accessing the entire equatorial circumference owing to their long light-delivery length (>7 cm), small thickness (<1.5 mm), elasticity, and flexibility, while their optical properties are optimized for efficient and homogeneous light delivery to scleral tissue. Using riboflavin and blue light (445 nm), we demonstrated SXL-induced stiffening of equatorial sclera around the entire circumference of fresh porcine eyeballs.

Methods

Elastomer Waveguide Fabrication

The waveguides were fabricated from polydimethylsiloxane (PDMS) elastomer material (Sylgard 184; Dow Corning, Midland, MI, USA). A base and curing solution was mixed at 10:1 ratio and added into a custom acrylic mold for preparing elastomer sheets approximately 20 cm × 20 cm. The solution was cured at room temperature for 48 hours, forming a solid, flexible elastomer sheet. The elastomer sheet was then wrapped in aluminum foil to facilitate cutting with a paper trimmer. The thickness of the elastomer sheet was determined by adjusting the total volume of solution used, and by inclining the mold to fabricate linearly tapered waveguides. We fabricated flat waveguides of thickness 0.8, 1.0, and 1.4 mm, with a fabrication error of approximately 0.1 mm. Our tapered waveguides had a thickness of 1.4 ± 0.1 mm at the proximal end, and a thickness of 0.5 ± 0.1 mm at z = 75 ± 5 mm. All of the waveguides were cut to a width of 5 mm, and had a typical length of 100 mm, of which ~70 to 80 mm was used to wrap the eyeball for SXL.

Waveguide Optical Characterization

To measure the optical transmittance of the elastomer material, the elastomer was cured in a 1-cm quartz cuvette. The transmittance was measured by using an Evolution 300 spectrophotometer (Thermo Scientific, Waltham, MA, USA). To quantify propagation loss, we coupled light into the elastomer waveguide by using a multimode fiber with a numerical aperture of 0.22 (Thorlabs, Newton, NJ, USA). The fiber was coupled to a diode-pumped solid-state laser delivering light at 445 nm (Civil Laser, Hangzhou, China). The fiber was stripped of the acrylate coating, and 2 to 3 mm of the bare fiber was inserted into the center of one end of an elastomer waveguide. To measure the propagation loss of the waveguides, the cut-back method was used. The transmitted power through the waveguide was measured while the waveguide was suspended in air, or placed on top of strips of scleral tissue dissected from fresh porcine eyeballs. The transmitted power through the waveguide was measured with a double-integrating sphere (IS200-4; Thorlabs) at waveguide lengths of 60, 45, 30, and 15 mm. The experiment was repeated with at least three waveguides for each thickness (0.8, 1.0, and 1.4 mm). The data were adjusted to compensate for material absorption and fit to an exponential decay model (see theory below) to extract the scattering loss coefficients to air and scleral tissue.

Waveguide Loss Model

A full derivation of this waveguide loss model is presented in Supplementary Note S1. In this simplified model, we consider waveguide propagation loss through three main mechanisms: material absorption, bulk scattering loss, and scattering due to surface roughness. The light intensity inside the waveguide $I_{in}(z)$ at position z along the length approximately follows an exponential decay:

$$I_{in}(z) \approx I_0 * e^{-(\alpha_{scatt}+\gamma)z}, \quad (1)$$

where γ is a loss coefficient due to material absorption, and α_{scatt} is a scattering coefficient describing total scattering loss (bulk + surface) resulting in incomplete total internal reflection.

Light extracted from the waveguide $I_{ext}(z)$ per unit length is described by:

$$I_{ext}(z) \approx \alpha_{scatt}(z) * I_{in}(z). \quad (2)$$

To compensate for the exponential attenuation in light delivery, one solution is to design the waveguide by varying the scattering cross-section α_{scatt} as a function of z. For uniform light delivery, we require $\frac{dI_{ext}}{dz} = 0$. For our waveguides, $\gamma \ll \alpha_{scatt}$ and $I_{in}>0$, this condition is achieved with the following expression[24] for α_{scatt}:

$$\alpha_{scatt}(z) \approx \frac{1}{C - z}, \quad (3)$$

where $C = 1/\alpha_{scatt}(0)$.

The scattering cross-section is inversely proportional to the thickness t of the waveguide, since the number of reflections per unit length increases with decreasing thickness.

$$\alpha_{scatt}(z) = \frac{A}{t(z)} \quad (4)$$

From Equations 3 and 4, the uniform delivery condition is satisfied with a linear taper given by:

$$t(z) \approx t_0 - Az, \quad (5)$$

where t_0 is the initial waveguide thickness at $z = 0$ and $A = t_0/C$.

Fluorescence Measurements

Fresh adult porcine eyes were obtained within 2 hours postmortem (Research 87, Inc., Boylston, MA, USA), and kept on ice during transport and storage before starting experiments. The whole eye was immersed in ~10 mL aqueous 0.5% riboflavin-5-monophosphate (Sigma-Aldrich Corp., St. Louis, MO, USA) for 30 minutes for staining. After staining, the eye

Investigative Ophthalmology & Visual Science

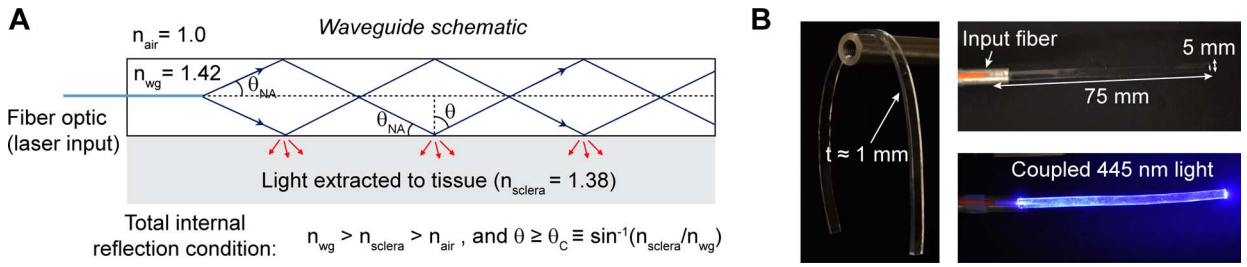

Figure 1. Elastomer waveguide schematic and optical characterization. (**A**) Schematic of the waveguide. Input light is delivered by an optical fiber (*blue line*) to the slab waveguide with effective refractive index n_{wg}. Optical rays greater than the critical angle $<\theta_C$ are guided via total internal reflection. In this case, part of the light is extracted to tissue primarily through surface scattering (*red arrows*). (**B**) Images of the flexible waveguide with coupled blue light through an input optical fiber.

was fixed on a rotational mount. For measurement of fluorescence distribution, a flat or tapered waveguide was wrapped around the eyeball equator. Blue light at low power (<1 mW) was coupled into the waveguide. Images were taken around the circumference of the eyeball by using a Nikon D90 camera (Nikon, Tokyo, Japan) with a 530 ± 25 nm bandpass emission filter (Edmund Optics, Barrington, NJ, USA) to collect the riboflavin fluorescence profile. The uniformity of the fluorescence distribution was quantified by the coefficient of variation, which is defined as the standard deviation divided by the mean light intensity along the waveguide. For photobleaching experiments, the camera was focused to one region of the sclera and images were taken every 30 seconds to capture the change in riboflavin fluorescence over time. The mean irradiance (measured in mW/cm^2) delivered by the waveguide was computed by measuring the input fiber power, the coupling efficiency (typically 60%–70%), and the waveguide dimensions.

Scleral Cross-Linking

SXL experiments were performed by using linearly tapered waveguides with thickness varying from 1.4 mm at the proximal end to 0.5 mm in the distal end. For consistency, the waveguides were wrapped around the eye equator such that the proximal end of the waveguide touches the major axis of the ellipsoid porcine cornea. The riboflavin-stained eyes were irradiated with 0, 25, or 50 mW/cm^2 for 30 minutes by using the waveguides or with direct illumination without the waveguide. At least six eyes were used for each condition. For direct illumination, a blue light–emitting diode (M455F; Thorlabs) was used as a light source and its divergent, incoherent light centered at 455 nm was gently collimated by a lens to a circular region of diameter ~15 mm in the equatorial sclera (see Fig. 6B). A humidifier (Optimus, Anaheim, CA, USA) was used to maintain scleral hydration during the SXL procedure. Following SXL, the eye was lightly labeled with a marker to indicate the location of the waveguide on the sclera, including the proximal and distal ends.

Tensiometry

The eye was roughly divided into four quadrants, beginning with the proximal end of the waveguide, and each measuring approximately 90° between the two axes of the ellipsoid porcine cornea. From the center of each quadrant, an anterior to posterior scleral strip was excised by using two parallel razor blades with a width of 4.9 mm. The retina was then removed, and the thickness at the irradiated area was determined by using a spring caliper. The sample was then clamped horizontally at a distance of 2.4 mm in anterior to posterior orientation between the two jaws of the tensiometer (Admet, Norwood, MA, USA). To expose the tissue to the physiological stress range as well as to establish the same initial conditions, a force of 30 mN was applied for 5 seconds. Afterwards in a second cycle, the force was reduced to 10 mN, at which the distance between the jaws was determined as the initial length (i.e., zero strain). After reaching 10 mN, the strain was increased linearly with a velocity of 0.017 mm/s and the force was measured every 10 ms until a force of 8 N was detected. Stress was calculated by dividing the force at a certain strain by the cross-section area of the sample (thickness obtained from caliper multiplied by width of 4.9 mm).

Statistics

Data were presented as mean ± standard deviation, unless otherwise stated. To assess differences between groups, two-tailed, unpaired Student's *t*-test was performed with significance set at $P < 0.05$.

Results

Waveguide Optical Characterization and Modeling

To achieve efficient light propagation inside the waveguide (Fig. 1A), the waveguide should have an effective refractive index higher than scleral tissue, which has a refractive index of ≈1.38. We fabricated flexible polymer waveguides by using PDMS elastomer, which has a refractive index of ≈1.42. To couple light into the waveguide, we used an input pigtail fiber with a numerical aperture of 0.22, which corresponds to incident angles above the critical angle (θ_C), enabling total internal reflection at either interface. The coupling efficiency of the fiber into the waveguide typically ranged between 60% and 70%. An image of the pigtail fiber–coupled waveguide is shown in Figure 1B. Typically, the dimensions of the waveguides were approximately 75 mm × 5 mm × 1 mm. The waveguides are highly transparent in the visible and near infrared wavelengths (400–800 nm), above 95% transmittance per centimeter (Fig. 2A). We measured the propagation loss of the waveguides while suspended in air and on excised scleral tissue for flat waveguides of different thicknesses. As expected, waveguide loss is inversely dependent on thickness (Fig. 2B). Fitting to Equation 1 yielded a scattering loss coefficient to air, α_{air} of (4.4 ± 0.2) × 10^{-3} mm^{-1}, and a scattering loss coefficient to scleral tissue, α_{sclera} of (5.9 ± 0.4) × 10^{-3} mm^{-1}. The waveguides had significantly higher loss to scleral tissue than to air ($P < 0.05$).

One strategy for compensating the exponential attenuation of light due to scattering loss is to taper the waveguide thickness. This waveguide geometry ensures fewer reflections toward the proximal end of the waveguide, where the

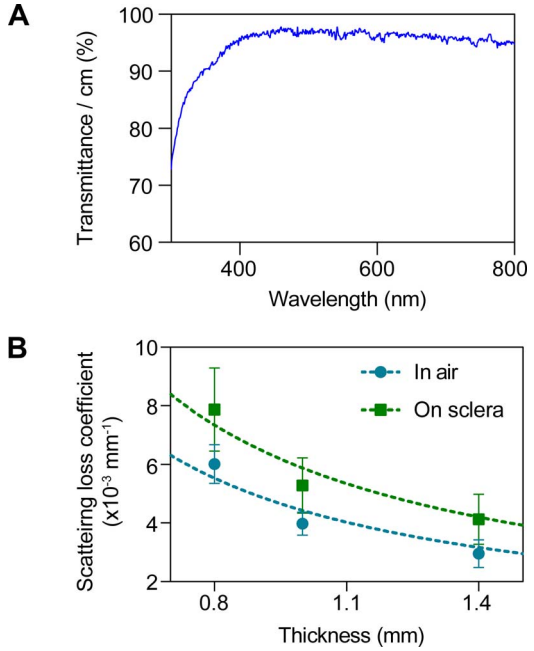

Figure 2. Optical characterization of the waveguides. (**A**) Optical transmittance of the waveguide measured in quartz cuvette. (**B**) Loss coefficient (α) to air and scleral tissue for flat waveguides of different thicknesses. Data are fit to $\alpha \sim 1/t$, showing that higher loss is achieved with thinner waveguides. The predicted propagation loss is 0.0044 mm^{-1} to air, and 0.0059 mm^{-1} to sclera, for a total loss of 0.0103 mm^{-1}.

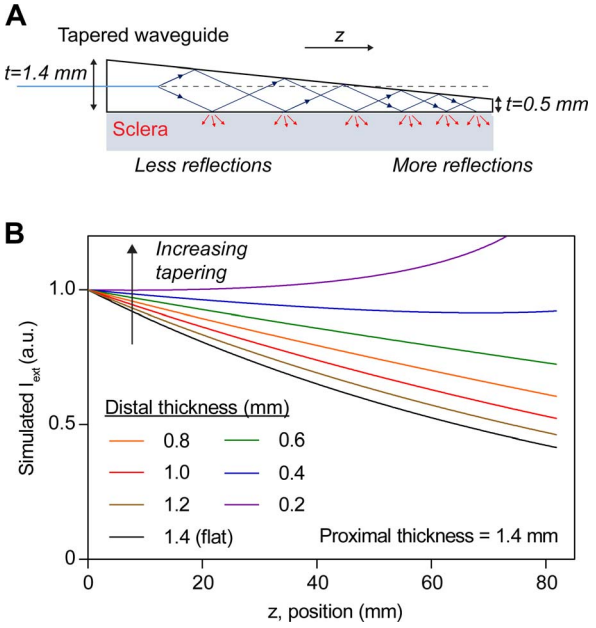

Figure 3. Tapering waveguides improve light uniformity. (**A**) Schematic of a tapered waveguide showing fewer reflections near the proximal end and more reflections near the distal end, compared to a waveguide of constant thickness. (**B**) Simulation of the light delivery profile along z for waveguides of different linear tapering. Waveguides of initial thickness of 1.4 mm at $z = 0$ were simulated by using Equation S9. Near-uniform light delivery is achieved for a waveguide with ~0.34-mm thickness at $z = 80$ mm.

thickness is larger, and more reflections toward the distal end where the thickness is smaller (Fig. 3A). Assuming absorption is much less than scattering loss, a linear taper ensures near-uniform light delivery (Equation 5). The light delivery profile into scleral tissue was simulated with Equation S9, using the empirically determined absorption and scattering loss coefficients (Fig. 3B). Increasing the tapering angle improves uniformity of light delivery for linearly tapered waveguides with $t_0 = 1.4$ mm until the thickness at the distal end is approximately 0.34 mm, at which point the tapering effect exceeds loss due to scattering and absorption.

Fluorescence Measurements on Riboflavin-Stained Eyes

To validate our theoretical results, we measured the fluorescence distribution from 0.5% riboflavin-stained porcine eyes by using waveguides wrapped around the equatorial sclera, and coupled 445-nm excitation light (Fig. 4A). The measured fluorescence profile around the eye is proportional to the excitation light extracted from the waveguide to the scleral tissue. We compared fluorescence profiles for flat and tapered waveguides (Fig. 4B). The profile for 1-mm-thick flat elastomers was fit to Equation 2, yielding a loss coefficient of 0.012 $\pm$ 0.001 mm^{-1}, in agreement with our previous measurement of propagation loss (Fig. 2B), which gave $\alpha_{air} + \alpha_{sclera} = 0.0103 \pm 0.0004$ mm^{-1}. When using tapered waveguides with a thickness of 1.4 to 0.5 mm, the fluorescence profile became more uniform, with a coefficient of variation of 9.9%, compared to 27.8% for the flat waveguides.

To verify the excitation of riboflavin in the sclera, we irradiated porcine eyes with mean irradiances of 25, 50, or 100 mW/cm^2 (Fig. 5) and monitored photobleaching-induced changes of riboflavin fluorescence during irradiation. We found that 25 mW/cm^2 was sufficient to bleach ~75% of the riboflavin fluorescence in 30 minutes.

Periscleral Cross-Linking

We performed SXL by using 445-nm light at irradiances of 0, 25, and 50 mW/cm^2 for 30 minutes on equatorial sclera around the entire circumference of the porcine eye. The efficacy of SXL-induced stiffening using the waveguides was compared with direct laser illumination of a single region (Fig. 6A). Stress-strain curves were obtained for excised scleral strips by using conventional tensiometry. Figure 6B shows there is no significant difference in stiffness when using the waveguide and direct illumination at the same mean light irradiance. The Young's modulus at 8% strain was 5.9 $\pm$ 0.5 MPa for nonirradiated sclera (Fig. 6B). SXL treatment at 25 mW/cm^2 resulted in a modulus of 9.5 $\pm$ 2.0 MPa for sclera treated with direct illumination, and 10.9 $\pm$ 1.2 MPa for sclera treated with waveguides. At 50 mW/cm^2, the modulus was 10.2 $\pm$ 1.9 MPa for direct illumination, and 10.7 $\pm$ 1.0 MPa with waveguides. SXL treatment in all cases resulted in an approximately 1.8-fold increase in the Young's modulus as compared to control eyes ($P < 0.001$). There was no significant difference in the Young's modulus for direct or waveguide-illuminated samples at either irradiance ($P > 0.05$). With the elastomer waveguide, there was no significant difference in stiffness between the proximally and distally treated halves of the sclera ($P = 0.28$ for 25 mW/cm^2, $P = 0.62$ for 50 mW/cm^2).

Discussion

In this study, we developed a novel approach to SXL by using flexible PDMS waveguides optimized for efficient and uniform light delivery to scleral tissue. The high optical transparency of

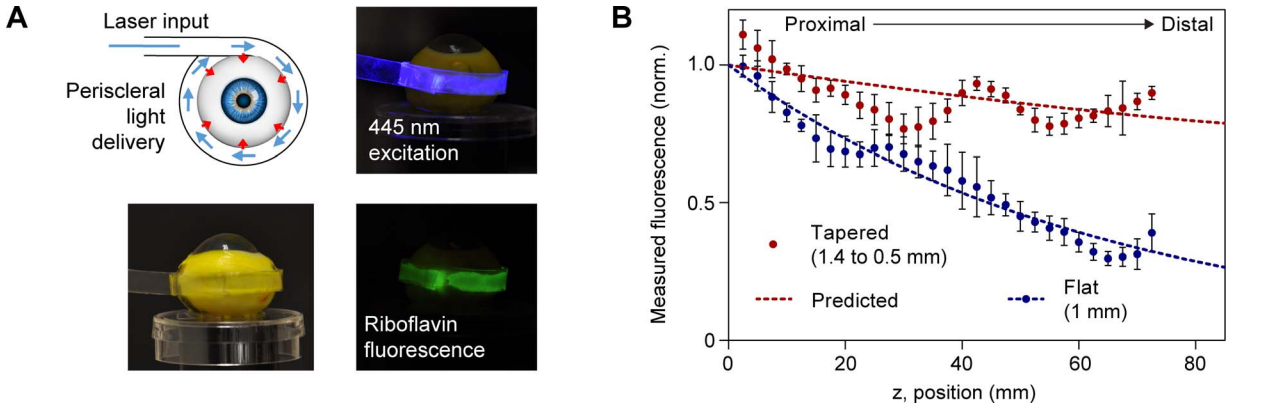

Figure 4. Experimental validation using tapered waveguides. (**A**) Measurement of fluorescence intensity around a riboflavin-stained eyeball, using coupled 445-nm light for excitation. (**B**) Fitting of light delivery profile for flat waveguides to Equation 2 (*dotted blue line*) yielding $\alpha_{scatt} = 0.012$ mm^{-1}. Predicted light delivery profile for tapered waveguide, using Equation 8 (*dotted red line*). Tapered waveguides show significantly more homogeneous light delivery than flat waveguides of similar mean thickness.

our waveguides (Fig. 2A) is well suited for SXL, since absorption-induced heat generation is minimal, in contrast to heat-generating active optical devices such as LEDs. Any wavelength in the visible to near-infrared region (400–800 nm) may also be used with the waveguides. For instance, Rose Bengal excitation using 532-nm green light is an alternative approach that could offer a different safety profile compared to that of riboflavin.[25] An attractive property of PDMS waveguides is their hydrophobic external surface, which prevents riboflavin diffusion into the waveguide throughout the procedure that may take at least 30 minutes.

Light leakage from the waveguides is achieved through bulk scattering inside the waveguide, and scattering due to surface roughness of the waveguide–sclera interface, and the waveguide–air interface. We found that light delivery to sclera was approximately 34% higher than to air, which is likely attributed to the higher surface roughness of the tissue (Fig. 2B). Another source of optical loss is radiation loss due to bending of the waveguide, which alters the total internal reflection angles. This effect was not significant in our study owing to the large radius of curvature of porcine or human eyes ($R \sim 12$ mm) compared to the waveguide thickness ($t \sim 1$ mm). The outer surface of the waveguide is surrounded by air, which has a much lower refractive index ($n = 1.0$) than PDMS ($n = 1.42$). Experimentally, we indeed observed similar overall propagation loss when the waveguide was placed flat on excised scleral strips (Fig. 2B) and when the waveguide was wrapped around the eye (Fig. 4B). In clinical practice, the waveguide is inserted into the extraocular socket and its external surface will be in contact with Tenon's capsule (with $n \sim 1.38$). To minimize optical loss to surrounding tissues, a reflective layer can be added to the outer surface of the waveguide, and a second, thinner layer of PDMS on top of that, ensuring tissue contacts only PDMS.

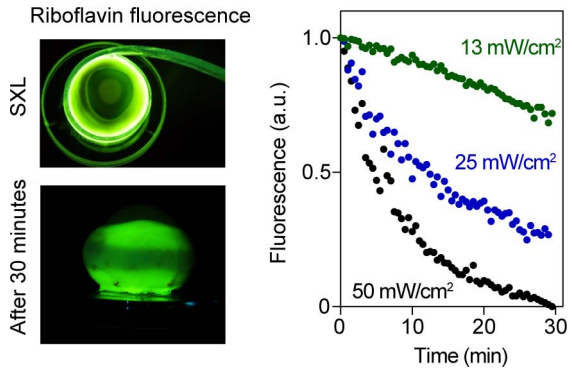

Figure 5. Photobleaching of riboflavin-stained sclera. *Left*: Images of porcine eyeballs during (*top*) and after (*bottom*) SXL with blue light. *Bottom image* shows pattern of bleached riboflavin along the equator after 30 minutes of irradiation. *Right*: Photobleaching of riboflavin, using mean irradiances of 13 to 50 mW/cm^2.

An important specification of our tapered waveguide design is the uniform light delivery profile into the sclera over the entire circumference, which has not been achieved in previous SXL experiments that target select regions of the sclera. As the rigid, outer layer of the eye, the sclera functions by resisting intraocular forces to maintain a fixed eye shape such that a stable retina image can be formed.[19] The sclera is also capable of undergoing matrix remodeling during normal growth, as well as pathologic myopia, resulting in axial elongation. While scleral stiffening with SXL may prevent axial elongation, uneven stiffening may cause significant tensions on the retina and probably transient astigmatism. For example, asymmetric placement of scleral buckles during retinal detachment surgery has induced transient astigmatic changes for at least 6 months following surgery.[26] In our study, we demonstrated significantly improved light uniformity by linearly tapering the waveguide thickness (Fig. 3). We achieved a variation in delivered light intensity of less than 10%, which may be further improved by increasing the tapering angle (Fig. 4). We also observed no statistically significant difference in the proximally and distally treated halves of the sclera as measured by tensiometry (Fig. 6B), suggesting light delivery is sufficiently uniform for whole-globe SXL. Another approach to improve the uniformity of light delivery would be to use two pigtail fibers to couple light into the waveguide from both sides (Supplementary Note S2). This approach is less attractive in practice, requiring fiber insertion and optimization of fiber–waveguide coupling at one end of the waveguide after it is wrapped around the eye.

Before SXL can be adopted in the clinic, risk of toxicities caused by riboflavin and light irradiation to ocular tissues must be considered. Using 450-nm blue light, a damage threshold of 200 to 400 mW/cm^2 for 20 minutes has been established for rabbit sclera.[21,27] In our study, we used 25 to 50 mW/cm^2 irradiation for 30 minutes, much lower than the damage threshold, and yet achieved an increase of greater than 80% in the Young's modulus at 8% strain. SXL-induced changes in elastic moduli can depend greatly on sample preparation and analysis procedure, but our results are generally consistent with previous studies using riboflavin and porcine eyes.[17,28,29]

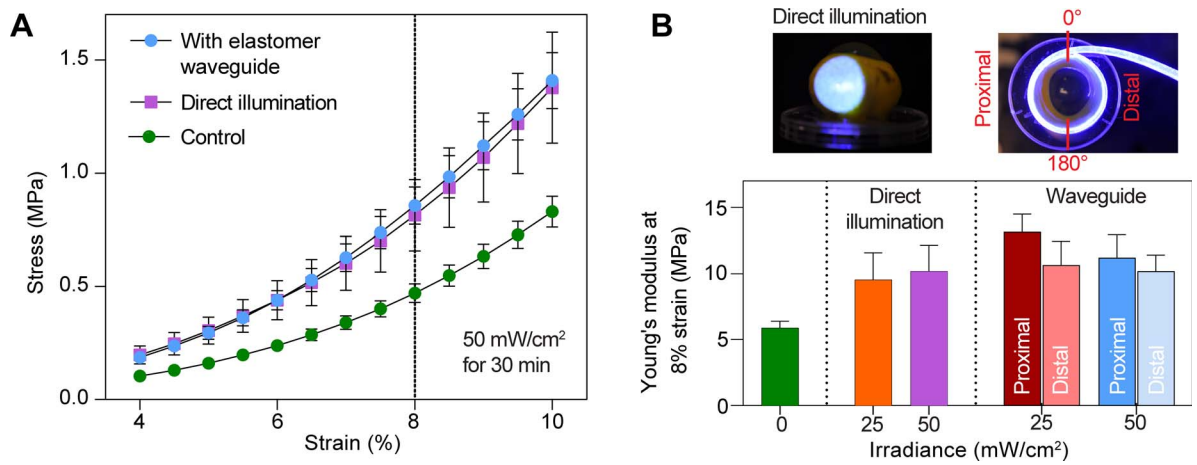

Figure 6. Stiffness of SXL-treated sclera. (**A**) Representative stress-strain curve obtained from tensiometry, comparing untreated sclera and cross-linked sclera, using elastomer waveguide and direct laser illumination. (**B**) Summary of data with at least six porcine eyes used for each group. The Young's modulus at 8% strain is reported as mean ± standard error. Using the waveguide, the stiffness of scleral tissues at the proximally and distally treated halves of the eye is not significantly different from each other and is similar to the positive control irradiated with direct illumination.

Light penetration into scleral tissue is limited by its high optical scattering properties; at 445 nm, the scattering coefficient[30] is ~80 cm–[1]. Factoring in riboflavin absorption (~135 cm^{-1} at 0.5% concentration), we anticipate cross-linking of less than 100 μm of scleral tissue in depth, much less than the full thickness (>350 μm).[31] Thus, our technique is unlikely to be affected by the variations in scleral thickness around the eye. Despite this limited therapeutic depth, we still achieved significant increases in overall scleral stiffness, measured by tensiometry. Of note, blue light is considered to be more efficacious than UV-A light for riboflavin-based SXL owing to its higher transmissivity and deeper penetration in tissue.[32] Preferential absorption of blue light over UV-A light by the choroid may also act as a barrier preventing retinal damage.[29] Biomechanical Brillouin imaging may be used to quantitatively assess the therapeutic depth of our technique, as well as validate the uniformity of stiffening around the sclera.[33,34]

As a proof of principle for inhibition of axial elongation, we chose to target equatorial sclera, which along with the posterior pole, are the most weakened scleral regions in myopia.[16,19] Similar reductions in both the number of cross-links[35] and extracellular matrix protein accumulation[36] in the equatorial and posterior regions of myopic sclera suggest SXL of either region may improve mechanical stability. Our flexible waveguides could also be used to access the posterior pole, which is more dramatically affected in later stages of myopia, typically resulting in significant thinning.[37,38] However, SXL of the posterior pole carries significant risk of phototoxicities to the retina and optic nerve, as well as the need for more invasive surgery to expose the posterior sclera. Furthermore, we anticipate SXL to be a prophylactic treatment for young, at-risk patients with high myopia before they develop severe consequences such as posterior staphyloma, which is more common in older patients (e.g., 50 years or older).[39]

To target the equator in vivo, our flexible waveguides may be safely inserted in Tenon's space underneath the rectus muscles, and wrapped around the eyeball. The surgical technique to enforce the equator is already clinically approved, for example, the cerclage technique for retinal detachment. Previously described SXL approaches use either a UV-A lamp,[40] a fiber-optic probe,[13,14] or a dental blue light source connected to plastic tubing[12,21] to deliver light to scleral tissue. Not only do these approaches provide uneven illumination by treating only a few target regions of the eye, but also the illumination area is relatively small owing to the limited probe size, typically covering an area of 10 to 100 mm^2. To treat the entire equatorial surface, the eyeball needs to be manually rotated to expose scleral tissue for optical access. Our waveguide approach enables simultaneous treatment of the entire circumference of the eye, improving treatment repeatability, and shortening overall procedure times significantly. Thirty minutes of light irradiation in our study was sufficient to cross-link an area spanning 75 × 5 mm, which can be easily adjusted depending on in vivo requirements. The significantly larger tissue volume that is cross-linked by our method could potentially have greater effects in halting axial growth of the eye. Another advantage of our technique over other methods of light delivery is the mechanical properties of our waveguides. Compared to harder, more rigid devices such as LEDs, or conventional fiber-optic probes to contact sclera, there is less risk of tissue trauma when using our thin, soft, and flexible PDMS-based waveguides.

In summary, periscleral cross-linking using flexible polymer waveguides can be used to stiffen scleral tissue with similar power efficacy as direct laser illumination. Our method provides several important advantages for clinical translation, including uniform light delivery, less invasive access to scleral tissue, and efficient cross-linking of a large area. In vivo studies are needed to demonstrate the safety of our method, as well as its long-term efficacy in inhibiting axial length elongation during myopia progression.

Acknowledgments

The authors thank Marleen Engler for technical assistance. They also thank Seonghoon Kim for useful discussions.

Supported by the National Institutes of Health (R01-EY025454, P41-EB015903), the National Science Foundation (CMMI-1562863), and the National Research Foundation of Korea (2016R1A6A3A11936389).

Disclosure: **S.J.J. Kwok**, P; **M. Kim**, P; **H.H. Lin**, None; **T.G. Seiler**, None; **E. Beck**, None; **P. Shao**, None; **I.E. Kochevar**, None; **T. Seiler**, None; **S.-H. Yun**, P

References

1. Dolgin E. The myopia boom. *Nature*. 2015;519:276–278.
2. Holden B, Sankaridurg P, Smith E, Aller T, Jong M, He M. Myopia, an underrated global challenge to vision: where the

current data takes us on myopia control. *Eye (Lond)*. 2014;28: 142–146.

3. Meng W, Butterworth J, Malecaze F, Calvas P. Axial length of myopia: a review of current research. *Ophthalmologica*. 2011;225:127–134.
4. Schultz DS, Lotz JC, Lee SM, Trinidad ML, Stewart JM. Structural factors that mediate scleral stiffness. *Invest Ophthalmol Vis Sci*. 2008;49:4232–4236.
5. Siegwart JTJ, Norton TT. Regulation of the mechanical properties of tree shrew sclera by the visual environment. *Vision Res*. 1999;39:387–407.
6. Ward B, Tarutta EP, Mayer MJ. The efficacy and safety of posterior pole buckles in the control of progressive high myopia. *Eye*. 2009;23:2169–2174.
7. Chen M, Dai J, Chu R, Qian Y. The efficacy and safety of modified Snyder-Thompson posterior scleral reinforcement in extensive high myopia of Chinese children. *Graefes Arch Clin Exp Ophthalmol*. 2013;251:2633–2638.
8. Curtin BJ, Whitmore WG. Long-term results of scleral reinforcement surgery. *Am J Ophthalmol*. 1987;103:544–548.
9. Ohno-Matsui K, Lai TYY, Lai CC, Cheung CMG. Updates of pathologic myopia. *Prog Retin Eye Res*. 2016;52:156–187.
10. Ohno-Matsui K. In: Spaide RF, Ohno-Matsui K, Yannuzzi LA, eds. *Pathologic Myopia*. New York: Springer Science & Business Media; 2013:354–360.
11. Wollensak G, Spoerl E, Seiler T. Riboflavin/ultraviolet-A-induced collagen crosslinking for the treatment of keratoconus. *Am J Ophthalmol*. 2003;135:620–627.
12. Iseli HP, Korber N, Koch C, et al. Scleral cross-linking by riboflavin and blue light application in young rabbits: damage threshold and eye growth inhibition. *Graefes Arch Clin Exp Ophthalmol*. 2016;254:109–122.
13. Liu S, Li S, Wang B, et al. Scleral cross-linking using riboflavin UVA irradiation for the prevention of myopia progression in a guinea pig model: blocked axial extension and altered scleral microstructure. *PLoS One*. 2016;11:e0165792.
14. Dotan A, Kremer I, Livnat T, Zigler A, Weinberger D, Bourla D. Scleral cross-linking using riboflavin and ultraviolet-A radiation for prevention of progressive myopia in a rabbit model. *Exp. Eye Res*. 2014;127:190–195.
15. Liu TX, Wang Z. Collagen crosslinking of porcine sclera using genipin. *Acta Ophthalmol*. 2013;91:253–257.
16. Wollensak G, Iomdina E. Long-term biomechanical properties of rabbit sclera after collagen crosslinking using riboflavin and ultraviolet A (UVA). *Acta Ophthalmol*. 2009;87:193–198.
17. Wollensak G, Spoerl E. Collagen crosslinking of human and porcine sclera. *J Cataract Refract Surg*. 20014;30:689–695.
18. Zhang M, Zou Y, Zhang F, Zhang X, Wang M. Efficacy of blue-light cross-linking on human scleral reinforcement. *Optom Vis Sci*. 2015;92:873–878.
19. McBrien NA, Gentle A. Role of the sclera in the development and pathological complications of myopia. *Prog Retin Eye Res*. 20013;22:307–338.
20. Zhang Y, Zou C, Liu L, et al. Effect of irradiation time on riboflavin-ultraviolet-A collagen crosslinking in rabbit sclera. *J Cataract Refract Surg*. 2013;39:1184–1189.
21. Iseli HP, Korber N, Karl A, et al. Damage threshold in adult rabbit eyes after scleral cross-linking by riboflavin/blue light application. *Exp Eye Res*. 2015;139:37–47.
22. Hafezi F, Richoz O. Scleral CXL to treat progressive myopia. *Cataract Refract Surg Today Eur*. 2015:1–2.
23. Yun SH, Kwok SJJ. Light in diagnosis, therapy and surgery. *Nat Biomed Eng*. 2017;1:8.
24. Nizamoglu S, Gather MC, Humar M, et al. Bioabsorbable polymer optical waveguides for deep-tissue photomedicine. *Nat Commun*. 2016;7:10374.
25. Cherfan D, Verter EE, Melki S, et al. Collagen cross-linking using rose bengal and green light to increase corneal stiffness. *Invest Ophthalmol Vis Sci*. 2013;54:3426–3433.
26. Hayashi H, Hayashi K, Nakao F, Hayashi F. Corneal shape changes after scleral buckling surgery. *Ophthalmology*. 2016; 104:831–837.
27. Karl A, Makarov FN, Koch C, et al. The ultrastructure of rabbit sclera after scleral crosslinking with riboflavin and blue light of different intensities. *Graefes Arch Clin Exp Ophthalmol*. 2016;254:1567–1577.
28. Zhang Y, Li Z, Liu L, Han X, Zhao X, Mu G. Comparison of riboflavin/ultraviolet-A cross-linking in porcine, rabbit, and human sclera. *Biomed Res Int*. 2014;2014:194204.
29. Iseli HP, Spoerl E, Wiedemann P, Krueger RR, Seiler T. Efficacy and safety of blue-light scleral cross-linking. *J Refract Surg*. 2008;24:S752–S755.
30. Nemati B, Rylander HG, Welch A. Optical properties of conjunctiva, sclera, and the ciliary body and their consequences for transscleral cyclophotocoagulation. *Appl Opt*. 1996;35:3321–3327.
31. Vurgese S, Panda-Jonas S, Jonas JB. Scleral thickness in human eyes. *PLoS One*. 2012;7:e296292.
32. Vogel A, Dlugos C, Nuffer R, Birngruber R. Optical properties of human sclera, and their consequnces for transscleral laser applications. *Lasers Surg Med*. 1991;11:331–340.
33. Scarcelli G, Kling S, Quijano E, Pineda R, Marcos S, Yun SH. Brillouin microscopy of collagen crosslinking: noncontact depth-dependent analysis of corneal elastic modulus. *Invest Ophthalmol Vis Sci*. 2013;54:1418–1425.
34. Kwok SJJ, Kuznetsov IA, Kim M, Choi M, Scarcelli G, Yun SH. Selective two-photon collagen crosslinking in situ measured by Brillouin microscopy. *Optica*. 2016;3:469.
35. Wollensak G, Iomdina E. Long-term biomechanical properties after collagen crosslinking of sclera using glyceraldehyde. *Acta Ophthalmol*. 2008;86:887–893.
36. Norton TT, Rada JA. Reduced extracellular matrix in mammalian sclera with induced myopia. *Vision Res*. 1995; 35:1271–1281.
37. Wollensak G, Iomdina E, Dittert DD, Salamatina O, Stoltenburg G. Cross-linking of scleral collagen in the rabbit using riboflavin and UVA. *Acta Ophthalmol Scand*. 2005;83:477–482.
38. Jonas JB, Xu L. Histological changes of high axial myopia. *Eye (Lond)*. 2014;28:113–117.
39. Hsiang HW, Ohno-Matsui K, Shimada N, et al. Clinical characteristics of posterior staphyloma in eyes with pathologic myopia. *Am J Ophthalmol*. 2008;146:102–110.
40. Wang M, Zhang F, Liu K, Zhao X. Safety evaluation of rabbit eyes on scleral collagen cross-linking by riboflavin and ultraviolet A. *Clin Exp Ophthalmol*. 2015;43:156–163.

Investigative Ophthalmology & Visual Science